J. Membrane Biol. 158, 187–196 (1997)

The Journal of
Membrane
Biology

A Model of Scorpion Toxin Binding to Voltage-gated K^+ Channels

G.M. Lipkind[1] H.A. Fozzard[2]

Departments of Biochemistry and Molecular Biology,[1] of Medicine,[2] and of the Pharmacological & Physiological Sciences, The University of Chicago, Chicago, IL 60637, USA

Received: 28 August 1996/Revised: 24 March 1997

Abstract. Mutational studies have identified part of the S5-S6 loop of voltage-dependent K^+ channels (P region) responsible for tetraethylammonium (TEA) block and permeation properties. Several scorpion peptide toxins — charybdotoxin (ChTX), kaliotoxin (KITX), and agitoxin (AgTX) — also block the channel with high affinity and specificity. Here, we examine the interaction predicted when the toxins are docked onto the molecular model of the K^+ channel pore that we recently proposed. Docking with the model of the Kv1.3 channel started by location of Lys-27 side chain into the central axis of the pore, followed by energy minimization. In the optimal arrangement, Arg-24 of KITX or AgTX forms a hydrogen bond with the Asp-386 carboxyl of one subunit, and Asn-30 is in immediate contact with Asp-386 of the opposing subunit in the tetramer. Toxin residues in proximity to the side chain of Lys-27 (Phe-25, Thr-36, Met-29, and Ser-11 in KITX) interact with the four C-end His-404s. For ChTX the interaction with Asp-386 is reduced, but this is compensated by additional nonbonded interactions formed by Tyr-36 and Arg-34. Comparison of calculated energy of interaction of these specific toxin-channel residues with experimental studies reveals good agreement. The similar total calculated energy of interaction is consistent with the similar IC_{50} for Kv1.3 block by KITX and AgTX. Steric contacts of residues in position 380 of the S5-P linker with residues on the upper part of toxins permit reconstruction of the K^+ channel outer vestibule walls, which are about 30 Å apart and about 9 Å high. Molecular modeling shows complementarity of the pore model to toxin spacial structures, and supports the proposal that the N-terminal borders of the P regions surround residues of their C-terminal halves.

Key words: Potassium channel—Scorpion toxins—Molecular models—Mutant cycle analysis—Point mutations

Correspondence to: H.A. Fozzard

Introduction

Voltage-gated K^+ channels are complex integral membrane proteins that form a gated transmembrane permeation pathway with almost perfect selectivity for K^+ (Pongs, 1992, 1993; Kukuljan, Labarca & Latorre, 1995). In spite of the absence of direct structural information from X-ray or NMR, investigators have made dramatic progress in our understanding of K^+ ion permeation and selectivity from high-resolution electrophysiological measurements, site-directed mutation of selected amino acid residues in the channel sequences, and molecular modeling.

Voltage-gated K^+ channels are composed of four subunits, each with 400–700 amino acids. Ideas derived from models that were based on the channel's primary structure (Guy & Seetharamulu, 1986) have led to the experimental identification of a highly homolgous 21 amino acid segment (P region), located between the fifth and sixth transmembrane segments, that participates in the permeation path and that contains binding sites for external and internal TEA block (MacKinnon & Yellen, 1990; Yellen, et al., 1991; Yool & Schwarz, 1991; Hartmann et al., 1991). Residues facing the aqueous solution of the K^+ channel pore have been identified by serial cysteine mutations, monitored by reaction with monovalent or divalent ions or formation of sulfhydryl bonds (Lü & Miller, 1995; Kürz et al., 1995; Pascual et al., 1995).

MacKinnon and Miller (1988) have pioneered in the use of a family of scorpion peptide toxins that occlude the pore to infer the structure of the channel's outer surface. These peptide toxins from scorpion venom have been used extensively in electrophysiological investigations of K^+ channels (Carbone et al., 1982; Possani, Martin & Svendensen, 1982; Miller et al., 1985). In contrast to the low millimolar affinity for TEA block, these scorpion toxins have pico- and nanomolar affinity for binding and block of the voltage-gated K^+ channels. Scorpion toxins are significantly larger than TEA, presum-

ably interacting broadly with the channel's outer mouth and occluding the outer entry to the channel pore (Anderson et al., 1988; MacKinnon & Miller, 1988; Miller, 1988; Park & Miller, 1992). A single toxin molecule interacts with the four subunits (Anderson et al., 1988; Goldstein & Miller, 1992; MacKinnon & Miller, 1988). Binding of the toxin is competitively antagonized by TEA (Miller, 1988), so TEA and the scorpion toxins bind to the pore in a mutually exclusive fashion (Goldstein & Miller, 1992). Using pairs of mutations of these toxins and the channel, a complementary binding surface for the structurally characterized toxins has been mapped, thereby locating several of the channel amino acids in space (Hidalgo & MacKinnon, 1995; Goldstein, Pheasant & Miller, 1994; Aiyar et al., 1995; Ranganathan, Lewis & MacKinnon, 1996; Naranjo & Miller, 1996).

We recently proposed a molecular model of the K^+ channel pore based on construction of inside and outside TEA binding sites and on pore mutations (Lipkind, Hanck & Fozzard, 1995). This model predicts a particular arrangement of the surface residues that are known to interact with the scorpion toxins. It should be possible to dock the structurally determined scorpion toxins onto the surface of the channel model. If an energetically plausible interaction occurs, then the apparent energies of interaction between specific toxin residues and corresponding channel residues could then be calculated and compared with the extensive experimental mutational data. If these calculations are plausible, then this approach may provide a guide to future experimental characterization of the channel surface, to understanding of the relative channel isoform and toxin analogue affinity differences, and to refinement of this and other models of the channel's surface.

Methods and Models

Modeling was accomplished in the Insight and Discover graphical environment (Biosym Technologies, San Diego, CA), as previously described (Lipkind & Fozzard, 1994; Lipkind et al., 1995). Molecular mechanics energetic calculations utilized the consistent valence force field approximation. For minimization procedures the steepest descents and conjugate gradients were used. For evaluation of electrostatic interactions with surface residues we used the experimentally derived macroscopic value of dielectric constant $D_{\text{eff}} = 31$ (Dudley et al., 1995).

Our previously reported K^+ channel pore model was developed for the Kv2.1 isoform (Lipkind et al., 1995). That isoform has low affinity for the scorpion toxins, but high affinity can be achieved by transfer of the S5-S6 segment containing the P region from a sensitive isoform to an insensitive one (Gross, Abramson & MacKinnon, 1994). Consequently, the residues in the model appropriate to Kv1.3 were substituted and the structure resubjected to energy minimization. No spacial change in the C^α positions of the surface residues resulted from these substitutions. Where the effects of specific mutations were investigated, the modified structures were again subjected to energy minimization. For comparison, the 21-residue P region alignments of the originally modeled Kv2.1, the lymphocyte Kv1.3 (Chandy & Gutman, 1995), and the Shaker proteins are shown.

```
                 361                 371                 381
                 ↓                   ↓                   ↓
Kv2.1      PASFWWATI TMTTVGYGDI YP
                 385                 395                 405
                 ↓                   ↓                   ↓
Kv1.3      PDAFWWAVV TMTTVGYGDM HP
                 430                 440                 450
                 ↓                   ↓                   ↓
Shaker B   PDAFWWAVV TMTTVGYGDM TP
```

Two features distinguish our model for the K^+ channel pore (Lipkind et al., 1995). Firstly, the P regions are extended nonregular hairpins with β-turns in the middle. Secondly, only the C-ends of the hairpins form the inner walls of the pore, with backbone carbonyl oxygens of the Gly-Tyr-Gly segments forming the selectivity filter of the channel. As a consequence of that structure, the N-ends are outside the pore, forming a radial arrangement of the loops. The four hairpins of the separate P loops were combined around two TEA molecules to form blocking complexes on the internal and external sides of the pore. In the outer vestibule of the modeled Kv2.1 channel, TEA was surrounded by the aromatic rings of four Tyr-380 residues. In this arrangement the N-terminal residues of the P loop, for example Asp-431 of Shaker or Asp-386 of Kv1.3, are also available for intermolecular interactions on the channel surface. It therefore appears that the triad of residues Asp-386, His-404, and Pro-405 from each subunit of the modeled Kv1.3, or their counterparts on the modeled Shaker, form a relatively flat surface on the outside of the pore that could be in close nonbonded contact with an interacting surface of the scorpion toxins. The critical surface residues of the Kv1.3 channel are shown in Fig. 1 in the locations predicted by the pore model, with subunits numbered I–IV for comparison with interacting toxin residues.

Miller (1995) has suggested a formal name for the class of scorpion toxins that block K^+ channels as ''α-K-toxins'' (α-KTX) and divided them into three subfamilies, as charybdotoxin (ChTX), noxiustoxin (NxTX), and kaliotoxin (KITX). All α-KTX have 37–39 amino acid residues with three conservative disulfide bonds that maintain the rigidity of the structures. The solution three-dimensional structures have been determined by multidimensional NMR and all show similar folding of the peptide backbone that includes one short α-helix (2-3 turns) and a three-stranded β-sheet (Bontems et al., 1991; Bontems et al., 1992; Krezel et al., 1995; Aiyar et al., 1995).

The toxin structures for this study were developed from the three-dimensional NMR structure of ChTX (Protein Data base code 1CRD). Because of their flexibility, the side chains facing the solution are less well defined by NMR, and these were located by energy minimization as described subsequently. As a test of this procedure, the spacial structure of KITX was initially based on the ChTX with a changed loop between residues 21–23 of KITX, which contains a deletion (AG-M) in place of the ChTX loop (LHNT). Comparison of this calculated structure with its NMR structure (*personal communication*, G. Gutman) shows coincidence of backbones, but the side chains of the critical

```
                  10                  20                  30
                  ↓                   ↓                   ↓
ChTX       ZFTNVSCTTS KE-CWSVCQRL H NT SRG-KCMNKKCRCYS
                  10                  20                  30
                  ↓                   ↓                   ↓
KITX       GVEI NVKCSGS P-QC LKPCKDA-GMRFG-KCMNRKCHCTPK
```

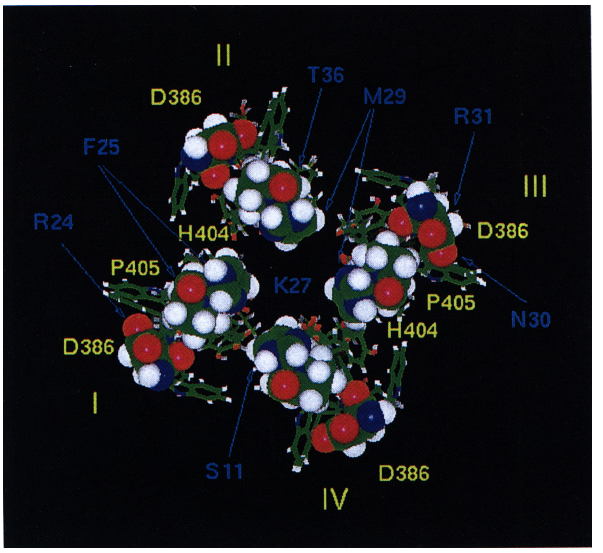

Fig. 1. The interactive surface of the Kv1.3 channel pore (the triad of residues Asp-386, His-404 and Pro-405 from each subunit) and the scheme of binding of KITX. The four subunits are arranged clockwise and numbered I–IV (top view). Positions of KITX residues are marked by blue arrows.

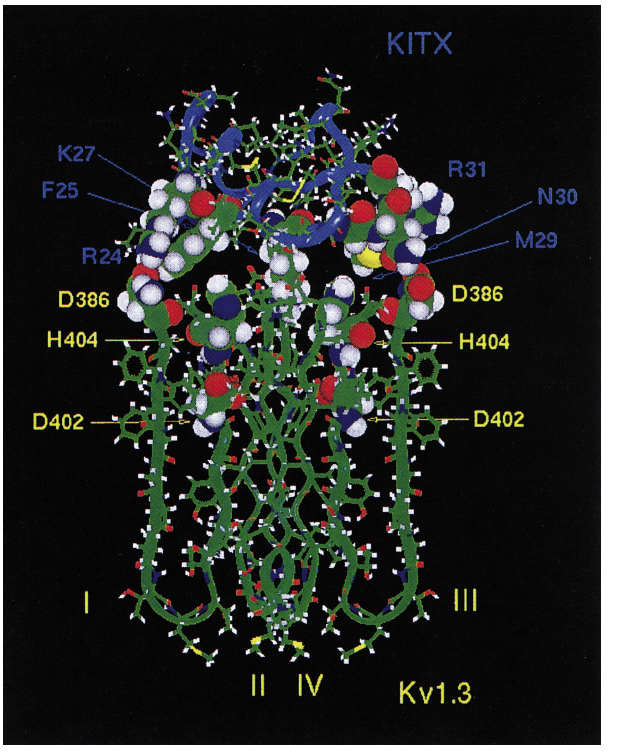

Fig. 2. Spacial model of the complex of KITX with the pore of Kv1.3 channel. Interacting residues of toxin and channel are shown by space-filling images and labeled by yellow and blue, correspondingly. The green ribbons represent the P regions of four subunits (I–IV), while the blue ribbon shows the backbone of KITX.

residues Arg-24 and Lys-27 (Hidalgo & MacKinnon, 1995; Goldstein et al., 1994) were oriented differently. Taking into account that Phe-25, Met-29, and Asn-30 form part of the interacting surface of the toxin (Ranganathan et al., 1996), we examined a blocking conformation of the toxin with the guanidinium group of Arg-24 located in a plane formed by side chains of the above three residues. In this case the angle of rotation around bond $C^{\alpha} - C^{\beta}$ of Arg-24 $\chi^1 = 180°$, instead of its value of −60° in the free toxin, and in this position Arg-24 does not interact with the C-end carboxyl of Lys-38. From the possible orientations of the flexible side chain of Lys-27 (Krezel et al., 1995), only in the case of $\chi^1(C^{\alpha} - C^{\beta}) = -60°$ is the vector $C^{\alpha} - N^{\gamma}$ perpendicular to the proposed interacting surface. Critical residues of the homologous ChTX do not coincide perfectly with those of KITX. In addition to Met-29, and Asn-30, two other residues − Arg-34 and Tyr-36 contribute to the interactive surface of the toxins and the overall binding energy (Goldstein et al., 1994; Naranjo & Miller, 1996). However, as in the case of KITX and AgTX, side chains of these residues also form a flat interactive surface of ChTX.

For purposes of calculation of an acceptable electrostatic field inside the pore during binding of α-KTX, the P regions were surrounded by hydrophobic segments S5 and S6 of the four subunits, in order to create a nonpolar environment. For simplicity the S5 residues (396–417) and the S6 residues (457–478) of Shaker (Guy & Conti, 1990) were modeled as poly-α-L-alanine α-helices, and located at distances of van der Waals contacts with the hairpins of the P region. The electrostatic fields were calculated using the DelPhi module. Dielectric constants were set to 10 for the protein and 80 for the solvent (Gilson & Honig, 1987).

Results

With the important residues known, the next step in characterizing the interacting surfaces is to identify pairs of residues, one each on the channel and the toxin, that interact with each other in the binding complex. Such contact partners allow the establishment of the toxin spacial arrangement with respect to the K^+ channel. For AgTX and KITX this problem has been considered through thermodynamic mutant cycles (Hidalgo & MacKinnon, 1995; Aiyar et al., 1995; Ranganathan et al., 1996). Mutagenesis of basic residues near critical residues in AgTX and some charged residues of Shaker has revealed one strongly coupled interaction — the mutation pair R24Q (toxin) — D431N (channel). Similar analysis also has established strong interaction of KITX with the identical residue Asp-386 of the Kv1.3 channel (Aiyar et al., 1995). Weak interaction has also been found for Arg-31 of AgTX with Asp-431 (Shaker), presumably on the opposite channel subunit (about 1 kcal/mol; Hidalgo & MacKinnon, 1995).

The extensive mutational data that have been accumulated on binding of α-KTX by K^+ channels invite analysis of the relative stereochemistry of their complexes. One framework for such an analysis is to dock the different toxins into our molecular model of the channel pore, which was constructed without the use of scorpion toxin interactions. We can then determine which pairs of toxin-channel residues are in proximity and re-

Table.

Interaction energy (kcal/mol)					Interaction energy (kcal/mol)	
Experimental	Model	KITX/AgTX residue	Kv1.3 model	ChTX residue	Model	Experimental[5]
−4.0[1,2]	−3.5	R24	D386(I)			
			D386(I),D386(II)	R25	−1.7	−1.5
			D386(II),D386(III)	R34	−1.6	−3.3
−1.0[1]	−1.0	R31	D386(III)	K31	−1.0	−1.0
−3.9[3]	−1.6(−2.6 to −3.1)[4]	N30	D386(III)	N30	−1.5(−2.5 to −3.0)[4]	−4.0
−3.9[3]	−4.0	K27	D402(×4)	K27	−4.0	−5.0
	−2.6	F25	H404(I),P405(I)	W14	−1.0	
	−1.0	T36	H404(II),P405(II)	Y36	−2.8	−3.1
−1.7[3]	−1 to −1.5	M29	H404(III),P405(III)	M29	−1 to −1.5	
	−1.4	S11	H404(IV),P405(IV)	S10	−1.4	
Total	−16.1 to −18.6				−16 to −18.5	
−1.1 to −2.0[2]	−1.9	F25	H404Y(I)			

[1] Hidalgo & MacKinnon, 1995
[2] Aiyer et al., 1995
[3] Ranganathan et al., 1996
[4] With estimate of a hydrogen bond energy of interaction in parentheses
[5] Goldstein et al., 1994

construct the interaction energy of the contacts between the α-KTX and K^+ channels.

Calculation of Interaction Energies for KITX and AgTX

Docking of KITX with the model of Kv1.3, having Asp-386 on the N-ends and His-404 on the C-ends, was achieved by positioning two contacts: the side chain of Lys-27 in its extended conformation into the central axis of the pore and the side chain of Arg-24 in close steric contact with the carboxyl group of Asp-386 of one of the subunits (designated as subunit I), in accordance with the data of Aiyar et al. (1995) and Hidalgo and MacKinnon (1995). After energetic optimization of the arrangement of KITX in this complex to avoid nonbonded repulsions of the interacting surfaces of KITX and the surface of the pore (Fig. 2), the energy of electrostatic interactions between the two charged residues was −3.5 kcal/mol. Experimental estimate of the energy of this interaction for KITX and AgTX is 4 kcal/mol (Aiyar et al., 1995; Hidalgo & MacKinnon, 1995), corresponding to formation of strong salt bridges between side chains of Arg-24 (toxin) and Asp-386 (channel). See the Table for specification of individual residue interactions between KITX, AgTX, and ChTX with Kv1.3, and for comparisons of model-derived and experimental energies of interaction.

The resulting configuration automatically places Arg-31 of KITX in proximity to Asp-386 of the P loop of the opposing subunit (subunit III) (Fig. 2). However, the distance between the side chains of Arg-31 and Asp-386 was sufficiently large in the model (~5Å) that the energy of electrostatic interaction was significantly weaker (about −1 kcal/mol). These evaluations are also in qualitative agreement with experimental data for the interactions of Arg-31 of AgTX with a Asp-431 residue of Shaker of −1.0 kcal/mol (Hidalgo & MacKinnon, 1995). In addition to the Arg-31 contact, the neighboring Asn-30 is in van der Waals contact with the same Asp-386 (Kv1.3) or Asp-431 (Shaker), and the energy of nonbonded interactions was estimated at −1.6 kcal/mol. Moreover, the neutral mutation N30A also decreases binding of AgTX by Shaker by almost 4 kcal/mol (Ranganathan et al., 1996), consistent with the presence of a hydrogen bond between side chains Asn-30 and Asp-431. In the force field cvff used in our calculation for the model, the formation of hydrogen bonds with noncharged donors or acceptors is not considered energetically. However, taking into account the energies of hydrogen bonds between amide groups in solutes of intermediate polarity of −1.0 to −1.5 kcal/mol (Klotz & Fransen, 1962), we can correct the energies of interaction between residues Asn-30 and Asp-386 for hydrogen bond formation, and these corrected values are noted parenthetically in the Table.

This binding of KITX with two Asp residues on the N-ends of opposing P loops also places some residues of KITX in proximity to the inner ring of four His-404 residues of the Kv1.3 channel pore. Phe-25, located near the Arg-24 to Asp-386 interaction, itself interacts with His-404 and Pro-405 of the same subunit (subunit I), and

Met-29 interacts with His-404 of the opposing subunit III. In each case the energy of nonbonded interactions equals −1 to −1.5 kcal/mol (Table). Proximity of Phe-25 of KITX to His-404 of Kv1.3 is shown by the studies of Aiyar et al. (1995), who estimated −1.1 to −2.0 kcal/mol interaction energy. Met-29 interaction was estimated by Ranganathan et al. (1996) to contribute about 1.7 kcal/mol to the AgTX-channel interaction. The molecular model also predicts that Ser-11 of KITX makes steric contacts with His-404 and Pro-405 of subunit IV (about −1.4 kcal/mol) and Thr-36 contacts His-404 of the opposing subunit II. Ranganathan et al. (1996) has shown experimentally that the two AgTX mutants S11A and T36A have reduced binding affinity to Shaker by 2.0 and 1.8 kcal/mol. Therefore, we see that the triad of residues Asp-386, His-404, and Pro-405 from each Kv1.3 subunit indeed forms an interactive surface on the outside of the pore of voltage-gated K^+ channels, which is in close stereochemical contact with the interacting surfaces of the α-KTX (Fig. 1).

In this orientation of KITX, substitution of His-404 of subunit I by Tyr creates a close and favorable perpendicular arrangement of the aromatic rings of residues Phe-25 of KITX and Tyr-404 of the channel. The energy difference of nonbonded interaction of the pair 25(KITX) − 404(channel) after mutation was 1.9 kcal/mol less. Experimentally, the mutation H404Y improved binding of KITX about 7-fold (Aiyar et al., 1995). We also think that the Phe-25 plays an important role in both binding of KITX and in restriction of the conformational freedom for the important side chain of Arg-24.

The distances separating residues of Arg-24, Lys-27, and Arg-31 of AgTX and KITX provide an estimate for spacing of the N-terminal Asp residues relative to the central axis of the pore. According to Hidalgo and MacKinnon (1995), the distance in Shaker from the center of the pore to Asp-431 is 12 to 15 Å (or 24–30 Å between Asp of opposing subunits). For Kv1.3 this distance from the pore center to Asp-386 is approximately 14–17 Å (Aiyar et al., 1995). In agreement with these experimental estimates, the calculated distance between Asp residues on the N-ends of the P loops in our model is 26–28 Å (Lipkind et al., 1995).

Calculation of Interaction Energies for ChTX

Docking of ChTX was achieved by superposition of ChTX on KITX, followed by optimization of the potential energy of the new complex. Because of differences in the structures of the two toxins, two strong interactions found for KITX (Arg-24 with Asp-386 and Phe-25 with His-404 of Kv1.3) are lost. However, these energetic losses are compensated by new interactions with specific bulky residues of ChTX — Tyr-36 and Arg-34, which substitute for smaller residues Thr-36 and His-34 of KITX. These two residues interact first of all with subunit II. The energies of interaction of Tyr-36 with His-404 and also with Pro-405 of subunit II of Kv1.3 are calculated to be −1.5 and −1.3 kcal/mol each (−2.8 kcal/mol together) (Table). The mutations of Goldstein et al. (1994) provide support for these interactions. In their experiments Y36N changed affinity by 3.1 kcal/mol. Arg-25 of ChTX also participates in weak electrostatic interactions with the Asp-386 residues of subunits I and II (about −0.8 kcal/mol each), while Arg-34 is interacting with Asp-386 of subunits II and III with similar energies. The mutation R25Q altered ChTX affinity to Shaker by +1.5 kcal/mol, while R34Q altered affinity by +3.3 kcal/mol (Goldstein et al., 1994). Asn-30 and Lys-31 also interacted with D386 of subunit III with about −1.5 (−2.5 to 3.5) kcal/mol and −1.0 kcal/mol, respectively (Table). Consistent with the proximity of these residues, the mutation K31Q reduces ChTX binding affinity by about 1.0 kcal/mol and N30D decreased binding by about 4 kcal/mol (Goldstein et al., 1994), presumably because of the electrostatic repulsion by the Asp residue added to loss of the binding energy. When we tested this mutation in the model (N30D) the change in the energy of electrostatic interaction was +2.5 kcal/mol.

Recently Naranjo and Miller (1996) have found another strong interaction between ChTX and the Shaker channel. The mutation M29I leads to a slight strengthening of block of wild-type Shaker channels, but the same mutation weakens block 1200-fold when tested on Shaker T449F. In the model of ChTX interaction with Kv1.3, mutual substitution of Met-29 by Ile and the four His-404 residues by Phe leads to immediate van der Waals contacts of the side chains of Ile-29 and Phe-404 of subunit III. However, very small rotation of toxin around the Lys-27 axis leads to significant repulsions with the aromatic ring of this residue, allowing an exact location of ChTX. The model also explains why all four subunits of Shaker must have the T449F mutation in order to block binding of ChTX (Naranjo & Miller, 1996). The proximity of the aromatic side chain of the channel at that position and residue 29 of the toxin is seen in Fig. 2. The model predicted a −1.0 to −1.5 kcal/mol interaction energy, compared to the experimental result of Goldstein et al. (1994) of −1.1 kcal/mol estimated from the mutation M29L. This example is understandable only if we assume that the α-K-toxin and K^+ channel interact as rigid bodies.

Two other interactions between ChTX and the channel can be identified in the model. After superposition of the two structures, Trp-14 and Ser-10 of ChTX are located in equivalent positions to Phe-25 and Ser-11 of KITX and AgTX. Trp-14 shows a small nonbonded energy of interaction with His-404 and Pro-405 of subunit I (−1.0 kcal/mol). Experimental substitution of Ala for

Trp-14 reduced ChTX affinity for Shaker by 0.6 kcal/mol (Goldstein et al., 1994). Ser-10 also shows a nonbonded interaction with H404 and P405 of subunit IV (−1.4 kcal/mol). Experimentally, the mutation S10A changed affinity for Shaker by 0.8 kcal/mol (Goldstein et al., 1994). The smaller experimental energy changes seen in the experiments probably reflects the presence of the smaller T449 in Shaker, rather than H404 of Kv1.3.

Consequently, the total energies of interaction for Kv1.3 block by KITX and ChTX at the mouth of the pore are similar (Table), consistent with the similar IC_{50} for Kv1.3 block by ChTX and KITX of 0.71 nM and 0.41 nM, respectively (Aiyar et al., 1995). For Shaker the presence of Thr-449 instead of His (in Kv1.3) is compensated by additional interactions of the toxins with the C-end residues of Pro-450. In Table the energies of interaction between specific residues on the interactive surfaces are presented, and the sums for the two types of toxins are similar. As a test of the accuracy of summing these individual residue-pair interaction energies and of their independence, we calculated the total energy of interaction between the molecules of KITX or ChTX with the Kv1.3 pore model in the energy minimized position. These also give similar values of −48 kcal/mol. This is larger than the sums in Table because it includes the distant electrostatic interactions of the entire charged toxins with the pore.

The estimates of residue interaction derived from mutational experiments are subject to varying uncertainty. Interactions of pairs of residues of ChTX and Shaker are the least reliable because they are based on changes of affinity from single mutations of either the toxin or the channel. However, our calculations support their interpretation as pairs of interactions between a residue of ChTX and 1–2 residues of the channel interactive surface. For KITX with Kv1.3 or AgTX with Shaker the experimental studies used mutant cycle analysis, which estimates more accurately the interaction of specific pairs of residues by reducing the influence of other residue and solute interactions. Although the similarity of energies calculated for KITX/AgTX and those from experiments by mutant cycle analysis could have resulted from offsetting errors, the agreement between the sums of individual interactions and the sums of the overall bimolecular interaction energies suggests that these errors are small.

Interaction of Lys-27 with the Channels

Widespread point mutations of ChTX have identified Lys-27 as a residue of special importance in toxin-channel recognition (Park & Miller, 1992; Goldstein & Miller, 1992; Goldstein et al., 1994; Stampe, Kolmakova & Miller, 1994). Replacement of Lys-27 with polar but uncharged Gln weakened ChTX affinity by nearly four orders of magnitude, and this residue is equally important for KITX and AgTX (Aiyar et al., 1995; Ranganathan et al., 1996). Moreover, position 27 is unique in another respect: neutral substitutions of Lys-27 make ChTX block completely insensitive to either internal K^+ or applied voltage (Goldstein & Miller, 1993). Lys-27 behaves as if 20% of the transmembrane potential field affects its binding. These facts support the original proposal of Goldstein and Miller 1993) that the side chain of Lys-27 enters into the pore, where it can interact with K^+ ions in the conduction path. The residue D447 (Shaker) or D402 (Kv1.3) is likely to contribute to the electrostatic interaction of Lys-27 with α-KTX. Mutation of this residue typically results in a nonfunctional channel (Goldstein et al., 1994). Pascual et al. (1995) were successful in obtaining measurable currents for Kv2.1 and significant loss of TEA sensitivity when two of the four subunits had neutral substitutions in this position. A similar wild type-D402N dimer of Kv1.3 was successfully made by Aiyar et al. (1996) and it reduced affinity for the toxin mutants with charged residues in position 27, but with relatively less effect on the wild type toxin.

The side chain of Lys-27 is located in the center of the model pore, interacting symmetrically with four His-404 of Kv3.1 with a nonbonded interaction energy of about −4 kcal/mol. The real value of this interaction is likely to be less than this, due to partial electrostatic repulsion between these residues. Although the side chain of Lys-27 is not in immediate steric contact with the four Asp residues (Fig. 2), the carboxyl groups create a strong negative field in the middle of the pore, providing recognition between the α-KTX and the K^+ channel by through-space electrostatic interactions with these four Asp residues, and the corresponding energy is calculated to be about −4 kcal/mol (Table). The loss of 3.9 kcal/mol of binding energy for the mutant K27M of AgTX (Ranganathan et al., 1996) and 5.0 kcal/mol for the mutant K27M of ChTX (Goldstein et al., 1994) could be interpreted as supporting the idea of electrostatic stabilization between Lys-27 and the Asp-402 residues. In support of the distant through-space electrostatic nature of this interaction, the size of the positively charged aliphatic side chain in position 27 of different derivatives of KITX has little effect on the binding affinity (Aiyar et al., 1995).

The α-KTX contain six basic amino acids in addition to Lys-27, and their association with the channel is aided by distant electrostatic interaction with the negatively charged surface of the K^+ channel (Goldstein et al., 1994; MacKinnon, Latorre & Miller, 1989; Nilius et al., 1985). We have calculated the electrostatic field for the complex of KITX with Kv1.3 (Fig. 3). The positive potential (blue contour) around KITX is surrounded by the negative electrostatic field (red contour) inside the pore. The correspondence of both fields shows that electrostatic forces at the molecular surface of the K^+ channel

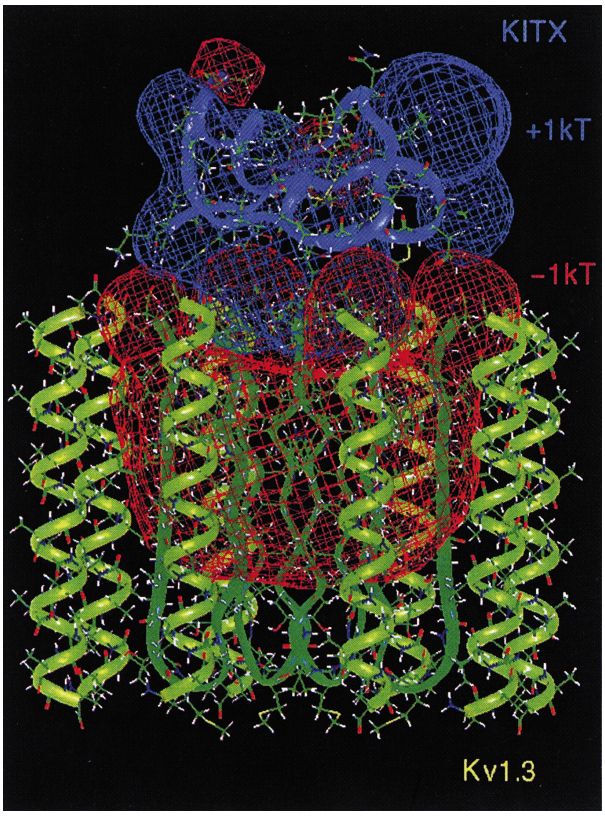

Fig. 3. The electrostatic fields in the complex of KITX with the model pore of the K^+ channel. Contours are shown at the 1 kT level with blue signifying positive and red signifying negative potentials. S5 and S6 segments are shown by light green ribbons.

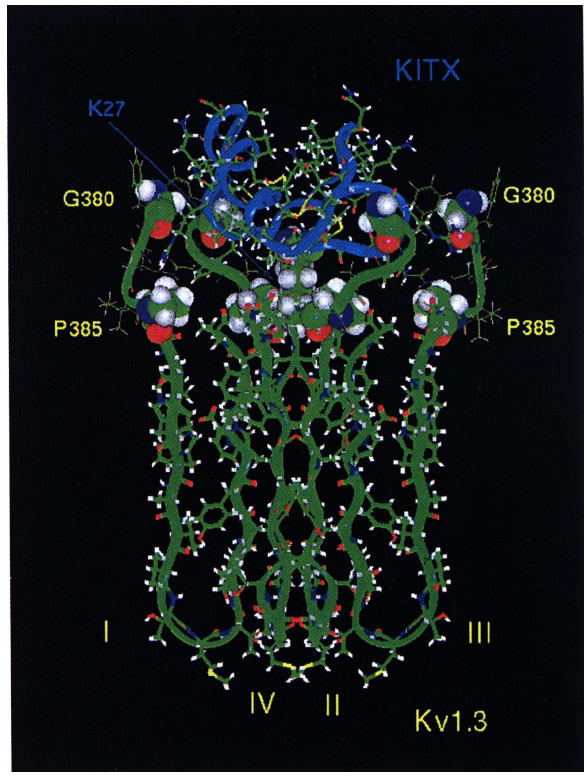

Fig. 4. Arrangement of four Gly-380 residues around KITX in its complex with Kv1.3 channel and nonregular strands of the sequences 380–386 (GFNSIPD) of four subunits in the outer vestibule added to the model of the K^+ channel pore.

may orient and hold a peptide toxin against the pore in the outer vestibule. Moreover, the K27E mutant of ChTX shows further reduction of binding with a $\Delta G = 6.7$ kcal/mol (Goldstein et al., 1994), as expected for a strong electrostatic interaction of the side chain of Lys-27 with the channel surface.

In this respect we are concerned about the new experimental results of Aiyar et al. (1996) showing equal sensitivity of wild type Kv1.3 and of the dimeric constructs of wild type-D402N for binding KITX. Neutralization of the other aspartic acids of the P region (D386N) had little effect on the binding of ChTX (Aiyar et al., 1995). In addition, mutant cycle analysis for the double mutation K27M-D431N shows independence of these residues for the binding of AgTX by Shaker (Hidalgo & MacKinnon, 1995). Both results suggest that D402/D431 is the single candidate for electrostatic interaction with Lys-27.

The Vestibule Outer Walls

One specific amino acid residue in the S5-P linker outside of the P region is in spacial proximity to molecules of the α-KTX, presumably by participating in formation of walls of the outer vestibule of the K^+ channel. This is Phe-425 of Shaker and Gly-380 of Kv1.3 in identical positions. Substitution of the bulky Phe-425 of Shaker by smaller residues, such as F425G, enhanced affinity of ChTX over three orders of magnitude (Goldstein et al., 1994). The sensitivity of Kv1.3 to inhibition by toxin progressively decreased as the size of the residue at position 380 increased (Aiyar et al., 1995), as if the inhibition was mediated by steric hindrance.

Comparative analysis of inhibition by different toxins has identified Trp-14 and Lys-31 of ChTX and Leu-15 and Arg-31 of KITX as candidates for interaction with Gly-380 of the two opposing subunits of Kv1.3 (Aiyar et al., 1995). In contrast, the mutation G380V had little influence on binding of NxTX, which has the small residues Ser and Gly in the equivalent positions. Another residue of ChTX, Thr-8, participates in close steric contact with one of the residues in position 425 of Shaker (Goldstein et al., 1994).

From the structure of ChTX it is seen that Trp-14, Thr-8, and Lys-31 are located on the outer edges of this molecule and they are approximately at equal distances from each other. Most likely, these residues interact

with positions 380 of Kv1.3 or 425 of Shaker of the three subunits I, III, and IV. Also we propose that another residue of ChTX — Ser-37 in the opposing position to Thr-8 — might interact with the remaining subunit II. In case of KITX the corresponding residues are Leu-15, Ser-9, Arg-31, and Pro-37. Location of these residues relative to the critical pore-interacting residues determines the necessary depth of the channel outer vestibule, which we estimate to be 8–9 Å. This suggestion allows reconstruction of one external loop of the outer funnel of the K^+ channel. For this effort we placed four residues of Val at the distances of close van der Waals contacts with residues Trp-14, Lys-31, Thr-8, and Ser-37 of ChTX or Leu-15, Arg-31, Ser-9, and Pro-37 of KITX in the toxin complex with the pore, because the mutation G380V eliminates binding of ChTX and KITX (Aiyar et al., 1995). Substitution of Gly for this Val determines the approximate arrangement of Gly-380 on the outer funnel walls of Kv1.3 (Fig. 4). Gly-380s of neighboring subunits are located at the distances 22–23 Å from each other with right counter-clockwise shift relative to four Asp-386 on the N-ends of the P loops.

In this arrangement the distance between C^α atoms of Gly-380 and Asp-386 of each subunit is 11 Å, which would correspond to the length of the sequence 380–386 of Kv1.3 if it were an α-helix. However, we think that this S5-P segment is not an α-helix, because that would direct the side chain of Pro-385 away from the pore. Pro-385 is likely to be directed toward the center of the pore, because when Cys is substituted in this position, interaction with small sulfhydryl reagents blocks current (Kürz et al., 1995). Rather than an α-helix, the peptide chain in the outer funnel walls probably adopts a nonregular conformation. A suggested conformation for the sequence 380–386 (GFNSIPD) that includes constraints on the location of Gly-380, Asp-386, and Pro-385 is shown in Fig. 4. Gly-380 of Kv1.3 and Phe-425 of Shaker determine the upper borders of the binding cavity (about 8–9 Å), because substitutions of residues beyond this segment on the N-terminal part of the S5-P linker by Lys do not influence the binding of α-K-toxins (Goldstein et al., 1994).

Discussion

The three types of experimental information that we used to develop our model of the Kv2.1 K^+ channel pore, in addition to the usual rules of protein structure, were (i) mutational study of the external and internal TEA binding/blocking sites in the closely related Kv isoforms, (ii) mutational study of channel permeation and selectivity, and (iii) outside accessibility to sulfhydryl-reactive agents of cysteine-substituted residue positions (Lipkind et al., 1995). Scorpion toxin binding/block and the mutational study of residues thought to be responsible for the toxin-channel interaction were not used in development of the model. However, the model did orient a set of residues on the surface of the pore that would be in proximity to a pore-occluding toxin molecule. We therefore sought to determine if the residue proximity found in the model would predict the energetics of toxin-channel recognition and binding.

The K^+ channel α-K-toxins are small enough to be structurally determined by NMR, providing excellent information on their backbone conformation, albeit with less constraint on the positions of their side chains. These toxins therefore provide a reasonable template for the channel surface. Mutant cycle analysis, a method developed by Fersht and colleagues (Carter et al., 1984; Schreiber & Fersht, 1995) to investigate interactions between individual pairs of residues, has the ability to define which residues on the ligand interact with which residues on the channel, although it too has limitations derived from multiple energetic effects of amino acid substitutions. Nevertheless, this method has placed a number of constraints on the structure of the channel outer surface.

The three residues (Asp-386, His-404, and Pro-405 in Kv1.3) of P regions from each subunit that are important for toxin interaction form an energetically plausible flat surface that places them in proximity to toxin residues of known importance. The residues on the N-end of the P region are located farther from the pore than those in the C-end, and the dimensions are approximately those predicted by mutational studies of the toxin-channel interaction, using the NMR structure of the toxin as calipers. In the model it is possible to calculate the energy of interaction between specific toxin residues and those on the channel. These calculations were compared with experimental measurements of change in toxin affinity by toxin and/or channel mutations. The agreement between the experimental and calculated values of interaction energies is quite good, considering the possible sources of error in such comparisons. The similar binding affinities for KITX/AgTX and ChTX is explained by different interactions that result in approximately the same energy of interaction.

It is important to underline that there are alternative spacial models and schemes of organization for the K^+ channel pore (Guy & Durell, 1995, 1996; Lü & Miller, 1995; Ranganathan et al., 1996; Pascual et al., 1995; Gross & MacKinnon, 1996; Aiyar et al., 1996). Several of these models have the critical channel-toxin residues in proximity. Some of the model differences reflect discrepancies that exist among the experimental data. For example, our model took advantage of the identification of exposed residues by their reactivity between substituted cysteines and sulfhydryl reagents by Kürz et al. (1995), a method pioneered for ion channels by Akabas

et al. (1992). Other investigators using similar techniques have reported conflicting results. For example, both Kürz et al. (1995) and Pascual et al. (1995) reported that I369 in Kv2.1 was not exposed to the outside solution, but Gross and MacKinnon (1996) and Lü and Miller (1995) found that V438 in an equivalent position in Shaker was reactive. A drawback of the cysteine substitution method is the possibility of a change in the basic structure by the substitution. This is suggested by the failure of many mutations to express currents when all four of the subunits contained the cysteine. Secondly, some of the mutant cycle data of Ranganathan et al. (1996) are difficult to reconcile with our model. In particular, the demonstration of direct interactions between K27 of AgTX and Y445 of Shaker, and G10 with T449, have led these investigators to propose a shallow external vestibule rather than a long narrow pore. Their conclusion is puzzling because of the choice of the conservative change of Y445 for Phe and the rather small value of the coupling energy (−1.5 kT). It is also difficult to reconcile this shallower pore with the need to select for TEA binding over tetramethylammonium and tetrapentylammonium (Heginbotham & MacKinnon, 1992) and for multiple K^+ binding sites in the voltage field (Stampe & Begenisich, 1996).

The estimates of atomic distances in the K^+ channel pore on the basis of cysteines and high-affinity metal binding sites (Krovitz, VanDongen & VanDongen, 1997) support our structural motif. These new data indicate that the outer vestibule of Kv2.1 has Tyr-380 residues on the outside, with Ile-379 residues located deeper and closer to the central axis of the pore. Substitution of I379 by Cys results in the formation of a Cd^{2+} coordination site. This makes it difficult for the Asp-378 or Asp-402 residues of Kv1.3 to be on the surface of the pore, as proposed by Aiyar et al. (1996), or for direct interaction of Lys-27 with Tyr-445 of Shaker (Durell & Guy, 1996).

In summary, a remarkable amount of insight into the structure of the K^+ channel pore has been developed in the few years since the Shaker channel was cloned. A particularly intriguing approach has been to use as structural templates the α-K-toxins, which block the pore by binding to its external mouth. This has shown that the channel has a rather wide vestibule about 10 Å deep and 25–30 Å wide. We have compared the available mutational data to our molecular model of the channel pore and find acceptable complementarity to the spacial structures of the α-K-toxins. The model makes energetically specific and testable predictions of interactions by toxin residues with specific channel subunits. In addition, the relative success of this effort suggests that other membrane protein surfaces might be explored by a similar interplay of mutation and molecular modeling.

References

Aiyar, J., Rizzi, J.P., Gutman, G.A., Chandy, K.G. 1996. The signature sequence of voltage-gated potassium channels projects into the external vestibule. *J. Biol. Chem.* **271:**31013–31016

Aiyar, J., Withka, J.M., Rizzi, J.P., Singleton, D.H., Andrews, G.C., Lin, W., Boyd, J., Hanson, D.C., Simon, M., Dethlefs, B., Lee, C.L., Hall, J.E., Gutman, G.A., Chandy, K.G. 1995. Topology of the pore-region of a K^+ channel revealed by the NMR-derived structures of scorpion toxins. *Neuron* **15:**1169–1181

Akabas, M., Stauffer, D., Xu, M., Karlin, A. 1992. Acetylcholine receptor channel structure probed in cysteine-substitution mutants. *Science* **258:**307–310

Anderson, C., MacKinnon, R., Smith, C., Miller, C. 1988. Charybdotoxin inhibition of Ca^{2+}-activated K^+ channels. Effects of channel gating, voltage, and ionic strength. *J. Gen. Physiol.* **91:**317–333

Bontems, F., Gilquin, B., Roumestand, C., Menez, A., Toma, F. 1992. Analysis of side-chain organization of a refined model of charybdotoxin: structural and functional implications. *Biochem.* **31:**7756–7764

Bontems, F., Roumestand, C., Gilquin, B., Menez, A., Toma, F. 1991. Refined structure of charybdotoxin common motifs in scorpion toxins and insect defenses. *Science* **254:**1521–1523

Carbone, E., Wanke, E., Prestipino, G., Possani, L.D., Maelicke, A. 1982. Selective blockade of voltage dependent K^+ channels by a novel scorpion toxin. *Nature* **296:**90–91

Carter, P.J., Winter, G., Wilkinson, A.J., Fersht, A.R. 1984. The use of double mutants to detect structural changes in the active site of the tyrosyl-tRNA synthetase (*Bacillus stearothermophilus*). *Cell* **38:**835–840

Chandy, K.G., Gutman, G.A. 1995. *In: Handbook of Receptors and Channels: Ligand- and Voltage-gated Ion Channels.* 1st ed., R.A. North, Editor. pp. 1–72. CRC Press, Boca Raton, FL

Dudley, S.C., Jr., Todt, H., Lipkind, G., Fozzard, H.A. 1995. A μ-conotoxin-insensitive Na^+ channel mutant: possible localization of a binding site at the outer vestibule. *Biophys. J.* **69:**1657–1665

Durell, S.R., Guy, H.R. 1996. Structural model of the outer vestibule and selectivity filter of the Shaker voltage-gated K^+ channel. *Neuropharmacology.* **35:**761–773

Gilson, M.K., Honig, B.M. 1987. Calculation of electrostatic potentials in an enzyme active site. *Nature* **330:**84–86

Goldstein, S.A.N., Miller, C. 1992. A point mutation in a Shaker K^+ channel changes its charybdotoxin binding site from low to high affinity. *Biophys. J.* **62:**5–7

Goldstein, S.A.N., Miller, C. 1993. Mechanism of charybdotoxin block of a voltage-gated K channel. *Biophys. J.* **65:**1613–1619

Goldstein, S.A.N., Pheasant, D.J., Miller, C. 1994. The charybdotoxin receptor of a Shaker K^+ channel: peptide and channel residues mediating molecular recognition. *Neuron* **12:**1377–1388

Gross, A., Abramson, T., MacKinnon, R. 1994. Transfer of the scorpion toxin receptor to an insensitive potassium channel. *Neuron* **13:**961–966

Gross, A., MacKinnon, R. 1996. Agitoxin footprinting the Shaker potassium channel pore. *Neuron* **16:**399–406

Guy, H.R., Conti, F. 1990. Pursuing the structure and function of voltage-gated channels. *TINS* **13:**201–206

Guy, H.R., Durell, S.R. 1995. *In: Ion Channels and Genetic Diseases.* D. Dawson, Editor. Rockefeller University Press, New York

Guy, R., Seetharamulu, P. 1986. Molecular model of the action potential sodium channel. *Proc. Natl. Acad. Sci., USA* **83:**508–512

Hartmann, H., Kirsch, G.E., Drewe, J.A., Taglialatela, M., Joho, R.H., Brown, A.M. 1991. Exchange of conduction pathways between two related K^+ channels. *Science* **251:**942–944

Heginbotham, L., MacKinnon, R. 1992. The aromatic binding site for tetraethylammonium ion on potassium channels. *Neuron.* **8:**483–491

Hidalgo, P., MacKinnon, R. 1995. Revealing the architecture of a K^+ channel pore through mutant cycles with a peptide inhibitor. *Science* **268:**307–310

Klotz, I.M., Fransen, J.S. 1962. Hydrogen bond between model peptide groups in solution. *J. Am. Chem. Soc.* **84:**3461–3466

Krezel, A., Kasibhatla, C., Hidalgo, P., MacKinnon, R., Wagner, G. 1995. Solution structure of the potassium channel inhibitor agitoxin 2: caliper for probing channel geometry. *Prot. Sci.* **4:**1478–1489

Krovitz, H.S., VanDongen, H.M.A., VanDongen, A.M.J. 1997. Atomic distance estimates from disulfides and high-affinity metal-binding sites in a K channel pore. *Biophys. J.* **72:**117–126

Kürz, L.L., Zuhlke, D., Zhang, H., Joho, R.H. 1995. Side chain accessibilities in the pore of a K^+ channel probed by sulfhydryl-specific reagents after cysteine-substitution mutagenesis. *Biophys. J.* **68:**900–905

Kukuljan, M., Labarca, P., Latorre, R. 1995. Molecular determinants of ion conduction and inactivation in K^+ channels. *Am. J. Physiol.* **268:**C535–C556

Lipkind, G.M., Fozzard, H.A. 1994. A structural model of the tetrodotoxin and saxitoxin binding site of the Na^+ channel. *Biophys. J.* **66:**1–13

Lipkind, G.M., Hanck, D.A. Fozzard, H.A. 1995. A structural motif for the voltage-gated potassium channel pore. *Proc. Natl. Acad. Sci., USA* **92:**9215–9219

Lü, Q., Miller, C. 1995. Silver as a probe of pore-forming residues in a potassium channel. *Science* **268:**304–307

MacKinnon, R., Latorre, R., Miller, C. 1989. Role of surface electrostatics in the operation of a high conductance Ca-activated K channel. *Biochem.* **28:**8092–8099

MacKinnon, R., Miller, C. 1988. Mechanism of charybdotoxin block of Ca^{2+}-activated K^+ channels. *Gen. Physiol.* **91:**335–349

MacKinnon, R., Yellen, G. 1990. Mutations affecting TEA blockade and ion permeation in voltage-activated K^+ channels. *Science* **250:**276–279

Miller, C. 1988. Competition for block of a Ca^{2+}-activated K^+ channel by charybdotoxin and tetraethylammonium. *Neuron* **1:**1003–1006

Miller, C. 1995. The charybdotoxin family of K^+ channel-blocking peptides. *Neuron* **15:**5–10

Miller, C., Maczydlowski, E., Latorre, R., Phillips, M. 1985. Charybdotoxin, a protein inhibitor of single Ca^{2+}-activated K^+ channels from mammalian skeletal muscle. *Nature* **313:**316–318

Naranjo, D., Miller, C. 1996. A strongly interacting pair of residues on the contact surface of charybdotoxin and a Shaker K^+ channel. *Neuron.* **16:**123–130

Nilius, B., Benndorf, K., Schuttler, K., Boldt, W. 1985. Use dependent depression of fast sodium current in heart muscle by the new antiarrhythmic substance Bonnecor (AWD 19-166, GS 015). *Pharmazie* **40:**852–854

Park, C.S., Miller, C. 1992. Mapping function to structure in a channel-blocking peptide: electrostatic mutants of charybdotoxin. *Biochem.* **31:**7749–7755

Pascual, J.M., Shieh, C.C., Kirsch, G.E., Brown, A.M. 1995. Multiple residues specify external tetraethylammonium blockade in voltage-gated potassium channels. *Biophys. J.* **69:**428–434

Pongs, O. 1992. Molecular biology of voltage-dependent potassium channels. *Physiol. Rev.* **72**(4):S69–S88

Pongs, O. 1993. Structure-function studies on the pore of potassium channels. *J. Membrane Biol.* **136:**1–8

Possani, L.D., Martin, B.M., Svendensen, I. 1982. The primary structure of noxiustoxin: a K channel blocking peptide, purified from the venom of the scorpion *Centruroides noxius hoffmann. Carlsberg Res. Commun.* **47:**285–289

Ranganathan, R., Lewis, J.H., MacKinnon, R. 1996. Spatial localization of the K^+ channel selectivity filter by mutant cycle-based structure analysis. *Neuron* **16:**131–139

Schreiber, G., Fersht, A.R. 1995. Energetics of protein-protein interactions: Analysis of the Barnase-Barstar interface by single mutations and double mutant cycles. *J. Molec. Biol.* **248:**478–486

Stampe, P., Begenisich, T. 1996. Unidirectional K^+ fluxes through recombinant Shaker potassium channels expressed in single *Xenopus* oocytes. *J. Gen. Physiol.* **107:**449–457

Stampe, P., Kolmakova-Partensky, L., Miller, C. 1994. Intimations of K^+ channel structure from a complete functional map of the molecular surface of charybdotoxin. *Biochemistry* **33:**443–450

Yellen, G., Jurman, M.E., Abramson, T., MacKinnon, R. 1991. Mutations affecting internal TEA blockade identify the probable pore-forming region of a K^+ channel. *Science* **251:**939–942

Yool, A.J., Schwarz, T.L. 1991. Alteration of ionic selectivity of a K^+ channel by mutation of the H5 region. *Nature* **349:**700–704